Achieving high-speed retraction in a stretchable hydrogel

Rosa Maria Badani Prado, Satish Mishra, Buckston Morgan, Rangana Wijayapala,

Seyed Meysam Hashemnejad, Santanu Kundu[*]

[1]Dave C. Swalm School of Chemical Engineering, 323 Presidents Circle, Mississippi State University, MS State, MS 39762, USA.

1   **ABSTRACT:** Hydrogels mimicking elastomeric biopolymers such as resilin, responsible for

2   power amplified activities in biological species necessary for locomotion, feeding, and defense,

3   can have applications in soft-robotics and prosthetics. Here, we report a bioinspired hydrogel

4   synthesized through a free radical polymerization reaction. By maintaining a balance between the

5   hydrophilic and hydrophobic components, we obtain gels with elastic modulus as high as 100 kPa,

6   stretchability up to 800%, and resilience up to 98%. Such properties enable these gels to catapult

7   projectiles. Further, these gels achieve a retraction velocity of 16 m s^{-1} with an acceleration of

8   4×10^3 m s^{-2} when released from a stretched state, and these values are comparable to those

9   observed in many biological species during the power amplification process. By utilizing and

10   tuning the simple synthetic strategy used here, these gels can be used in soft robotics, prosthetics,

11   and engineered devices where power amplification is desired.

12

1   Introduction

2   Elastomeric biopolymers such as resilin play a vital role in dictating the power amplification

3   process.[1–4] Biological species perform some remarkable activities necessary for locomotion,

4   feeding, and defense.[5] Many of these activities include a power amplification mechanism, in which

5   a particular biological system rapidly releases stored-energy by achieving a very high velocity over

6   a short period of time, resulting in high power output. Such power amplification allows insects

7   such as locust to jump and Mantis shrimp to kill prey by its appendage strike.[5,6] These elastic

8   biopolymers display high and reversible stretchability with low energy dissipation –typically

9   characterized as high resilience– and rapidly retract to their original dimensions after the removal

10   of mechanical load.[1,7] Specifically, resilin displays up to 300% stretchability and high resilience,

11   as >90% of the applied energy stored during deformation is recovered.[1,3,4] Such remarkable

12   properties of resilin have been attributed to a balanced combination of entropic and enthalpic

13   elasticity originated from the presence of hydrophilic (exon I) and hydrophobic (exon III) segments

14   in resilin.[1–4]

15   A reasonably good understanding regarding the origin of elasticity in elastomeric biomaterials

16   allows us to engineer materials mimicking some characteristics of those biomaterials. There are

17   many potential applications, viz. in artificial muscles, prosthetic devices for assisting people with

18   restricted mobility, energy harvesting, and enabling soft-robots for power amplification.[8] Since

19   hydrogels are the natural choice of mimicking water containing biomaterials, there are numerous

20   efforts in developing highly stretchable and resilient hydrogels.[9,10] However, some of these

21   hydrogels are based on recombinant proteins, therefore, obtaining a significant amount of such

22   materials for practical applications is challenging.[1,11] There also have been efforts to synthesize

23   polymeric hydrogels with high stretchability and resilience, but many of the synthesis schemes

1   require complex reaction routes that limit their large-scale applicability.[9,10,12–14] Furthermore,

2   although many of these systems display high stretchability, a significant energy dissipation during

3   cyclic loading is observed.[9,10,12–14] None of these hydrogels have been tested for the retraction

4   behavior from a stretched state, however, the dissipation of energy observed in these gels is

5   expected to cause a lower retraction velocity, which will defeat the very purpose of their

6   applications for power amplification.

7   Here, we report a highly stretchable and resilient hydrogel that displays a very high retraction

8   velocity gained over a short period of time, i.e. with high acceleration, after released from a

9   stretched state. The hydrogels are synthesized through a simple reaction scheme involving free-

10   radical copolymerization of acrylic acid (AAc), methacrylamide (MAM), and poly(propylene

11   glycol) diacrylate (PPGDA) using potassium persulfate (KPS) as an initiator. To the best of our

12   knowledge, a hydrogel capable of achieving such high retraction velocity and acceleration has not

13   been reported in the literature. Because of these attributes, these hydrogels have been demonstrated

14   to catapult projectiles over a long-distance.

15

16   **Experimental Section**

17   **Materials.** To synthesize the gels in this study, we have used poly(propylene glycol) diacrylate

18   (PPGDA) with a molecular weight of 800 g mol^{-1}, sodium dodecyl sulfate (SDS, 98.5%), acrylic

19   acid (AAc, 99%), methacrylamide (MAM, 98%), and potassium persulfate (KPS, 99%). All these

20   chemicals were obtained from Sigma Aldrich and used as received. Sodium chloride (NaCl,

21   99.9%) was purchased from Fisher Scientific and was used as received. For all experiments,

22   deionized water of resistivity 18.2 mΩ was used.

23   **Hydrogel Synthesis.** The gel samples were synthesized with different concentrations of

24   monomers (AAc and MAM). The nomenclature used for the gels (17%-, 27%-, 37%-Gels)

indicates the total concentration of the monomers (g mL^{-1}) used to synthesize the gels. First, aqueous 0.8 M NaCl solution was prepared. 83 mL of saline solution was mixed with 7% (g ml^{-1}) of SDS, considering 100 mL as the volume basis. The solution was stirred using a magnetic stirrer at 220 rpm for approximately 30 min in a warm water bath maintained at 55 °C until a clear solution was observed. The desired amount of monomer mixture was prepared separately by adding MAM into AAc, maintaining a weight ratio of MAM to AAc as 1:4, and considering 100 mL as a basis for the calculation. The monomer mixture was mixed for approximately 15 min at 220 rpm using a magnetic stirrer at room temperature (22 °C). The clear solution of SDS in saline water was taken out from the warm water bath and mixed with 1% (g g^{-1}) of PPGDA using the monomer mixture weight as a reference. This solution was mixed for 5 min using a magnetic stirrer at 220 rpm. After mixing, the monomer mixture was added dropwise to this solution and stirred for an additional 5 minutes to obtain a mixture of reactants. 0.2% (g g^{-1}) of KPS was prepared, considering the monomer mixture as a basis, added into 17 mL of saline solution, and stirred for 5 min. The KPS solution was added dropwise to the reactant mixture while stirring it at 220 rpm. The final transparent solution was poured in an airtight glass container and placed in a water bath at 75 °C for 2 h to obtain a translucent gel. The containers used to cast the gels were a 2 L bottle, 5 mL vials, and 5-mm-diameter glass tubes. Once the gels formed, the heat source was turned off, and the water bath was allowed to cool down for the next 24 h before samples were used for further testing.

Swelling Experiments. For the swelling tests, small cubic samples (10×10×10 mm^3) were weighed, dried in a vacuum oven (≈226 torr) for 72 h at room temperature, and weighed again to determine the water loss. The water content in the as-prepared gels was estimated as the change in the gel weight after drying with respect to the initial sample weight. Next, the samples were

1   immersed in 50 mL of DI water for 24 h to swell. The swelling ratio (g g^{-1}) was obtained as a ratio

2   of sample weight after swelling to the dry weight.

3   **Tensile testing.** All mechanical tests were performed at room temperature (22 °C). A custom-

4   built setup was used for conducting the tensile experiments, and the details regarding the

5   experimental setup and data analysis protocol can be found in our previous publications.[15,16] In

6   these experiments, a dogbone-shaped gel sample was prepared by cutting from the gel-sheet using

7   a 3D-printed punch. The dogbone sample had a gauge length of 4.2 mm, breadth of 4.2 mm, and

8   an approximate thickness of 9.5 mm. The dogbone sample was held by the four supporting pins

9   fixed to the top and bottom support blocks. A clamp was attached at the top and bottom blocks to

10   avoid the sample slippage. The sample was stretched by moving the top supporting block using a

11   moving stage (M414.3PD, Physik Instrumente). The sample was stretched with the stage velocity

12   of 1 mm s^{-1} (strain-rate ($\dot{\varepsilon}$) of 0.048 s^{-1}) until the failure of gel occurred. The setup was controlled

13   by a custom-built program in NI LabVIEW framework. During the sample stretching, images were

14   taken by a monochrome camera (Grasshopper3, Point Grey Research Inc.) at ≈16 fps. Every

15   sample was marked with three lines (1,2,3) at the gauge region to calculate strain (ε) and $\dot{\varepsilon}$ by

16   using a custom-built image-processing program in MATLAB. Here, ε represents the average of

17   the change in distance between lines 1-2, 2-3, and 1-3, normalized by their initial distances. The

18   corresponding stretch ratio, λ, can be estimated as ε+1. The force value corresponding to an

19   applied stretch is measured by the deflection of a cantilever with a known stiffness. Nominal stress

20   (σ) was estimated by dividing the measured force with the initial cross-sectional area of the gauge

21   region of the sample.

22   **Cyclic loading and determining resilience.** Cyclic loading experiments were also performed

23   using the custom-built setup described above. In these experiments, samples were stretched with

1   the same strain-rate ($\dot{\varepsilon}$) of 0.048 s^{-1} until those experienced the prescribed nominal stress (σ).

2   After the prescribed stress was attained, the samples were unloaded with the same strain-rate until

3   the stress became zero. The applied strain and strain-rates were determined from the images as

4   described above in the tensile testing section.

5   **Retraction experiments.** For the retraction experiments, a gel string sample with a diameter of

6   4 mm and a length of 45 mm was clamped at both ends on the tensile testing setup. The sample

7   was then stretched, and stretch ratios of λ =3, 4, 5, and 6 were considered. The sample was then

8   marked with seven equidistant lines that were tracked during the retraction process, as described

9   below. The string was cut with scissors adjacent to the bottom clamp and was allowed to retract.

10   The retraction process was recorded by using a high-speed camera (Miro M310, Phantom) at

11   ≈5000 fps. The images were analyzed using a custom-developed image-processing program in

12   MATLAB. The data was used from the time at which the string was snapped. While retracting,

13   the string slacks as soon as it crosses its initial length. The data after slack-time was not used for

14   analysis.

15   To calculate the velocity of each marked line, a fifth-order of Fourier series was used to fit the

16   position (*f*) vs. time (*t*) data, which can be mathematically represented as,

17   $f(t) = a_0 + \sum_{i=1}^{5} a_i \cos(\omega t) + \sum_{i=1}^{5} b_i \sin(\omega t)$, where a_0, a_is, b_is, and ω are the fitting parameters. The

18   resultant function was then differentiated to obtain the velocity. The differentiation of the above

19   equation can be mathematically expressed as, $\dfrac{df(t)}{dt} = \omega\left(-\sum_{i=1}^{5} a_i \sin(\omega t) + \sum_{i=1}^{5} b_i \cos(\omega t)\right)$. The

20   expression was further differentiated to estimate the acceleration, which can be mathematically

21   represented as, $\dfrac{d^2 f(t)}{dt^2} = -(\omega)^2\left(\sum_{i=1}^{5} a_i \cos(\omega t) + \sum_{i=1}^{5} b_i \sin(\omega t)\right)$.

Results and discussion

Hydrogel synthesis. As displayed in Figure 1A, upon chemical reaction, AAc and MAM form hydrophilic poly(acrylic acid) (PAAc) and poly(methacrylamide) (PMAM) chains. The hydrophobic PPGDA chains connect the PAAc and PMAM chains forming crosslinks. Figure 1B represents a schematic of the proposed network structure of the gel. Note that PPGDA chains can also polymerize as a result of the free radical reaction, leading to a significant distribution in their molecular weight. Because of hydrophobicity, the poly(propylene glycol) (PPG) blocks collapse, and multiple of these blocks can associate forming hydrophobic aggregates. The surfactant SDS in the NaCl reaction media promotes the formation of these hydrophobic aggregates.[17] The gels are opaque, indicating a phase-separated structure.

Previously, gels were synthesized by using free-radical polymerization of acrylic acid (AAc), methacrylamide (MAM), and copolymerization of AAc and MAM, and in many cases N,N'-methylenebisacrylamide was used as a crosslinker.[18–21] These gels have displayed high water swelling capabilities. In a limited number of studies, hydrophobic chains have also been incorporated.[22,23] High stretchability has also been reported in a few studies, but that can be associated with hysteresis.[19,22] The PPG or poly(propylene oxide) present in the PPGDA becomes hydrophobic with increasing temperature, and such property has been harnessed to obtain well-known pluronic hydrogels.[24] In our synthesis scheme, hydrophobic PPGDA has been introduced in the gel network to maintain a balance with hydrophilic PAAc and PMAM. As a result, hydrogels with high stretchability and resilience, capable of performing power amplified activities, were obtained.

For the present study, we have considered 17%, 27%, and 37% (g mL^{-1}) total monomer (MAM and AAc) concentration while keeping a constant MAM to AAc weight ratio of 1:4. A fixed

1   proportion of KPS (0.2% (g g^{-1})) and PPGDA (1% (g g^{-1})) with respect to the total monomer weight

2   was used for each gel. The FTIR results of the synthesized gel capture the copolymerization of the

3   monomers (see Supporting Information, Figure S1). Based on the monomer concentration, these

4   gels are referred to as 17%-, 27%-, and 37%-Gels throughout this article. The water content of the

5   as-prepared 17%-, 27%-, and 37%-Gels has been determined as 80.9±0.9%, 67.6±0.2%, and

6   64.9±0.1%, respectively, by drying the gel samples in a vacuum oven for 72 h at room temperature

7   (Figure S2A-B and Table S1). During gel formation, we have observed some level of syneresis for

8   the 17%- and 27%-Gels likely related to the presence of hydrophobic monomers, therefore, the

9   polymer concentrations in those gels have been found to be slightly higher than the monomer

10   concentration in the initial solution.

11   No significant additional swelling was observed when the as-prepared samples were stored in a

12   0.8 M aqueous NaCl solution. However, submerging the samples in water results in significant

13   swelling. Specifically, the dried 17%-, 27%-, and 37%-Gel samples immersed in water for 24 h

14   can absorb water ≈87.9±14.9, 44.2±1.4, and 34.6±0.1 times of their dry weight, respectively

15   (Figure S2C and Table S1). The water absorbance capacity of our gel is higher than that of PAAc-

16   PMAM hydrogels,[25] however, it is comparable to that of acrylamide-based polyampholyte

17   hydrogels.[26] High water absorption capacity in our gels can be related to their synthesis conditions.

18   The presence of cations from NaCl screens the acid groups of AAc from ionization,[25] as a result,

19   the swelling of the synthesized gel is relatively lower. However, when the samples are submerged

20   in water, NaCl salts leach out, resulting in ionization of acid groups and the corresponding increase

21   of water uptake. We have found that the samples are stable in NaCl solution, even for months,

22   therefore, these gels can be used in a saline environment. In this study, we have considered the as-

23   prepared samples for further testing. As the gels display a significant swelling capacity when

submerged in water, it can be hypothesized that the polymer chains are loosely crosslinked, with high molecular weight strands between the crosslinks that can be extended significantly during the mechanical stretching as discussed below.

The structure of our gels can be compared with resilin, a disorderly protein that consists of both hydrophilic and hydrophobic segments.[3] At low strain, the resilin elasticity is governed by the entropic stretching of hydrophilic segments (exon I).[1–4] In contrast, the high-strain response is primarily governed by the stretching of hydrophobic segments (exon III).[1–4] The hydrophobic content dictates the water content in the gel, therefore, affects the modulus of the material. The power amplification mechanism in many biological systems can be attributed to the rapid retraction response of resilin from a stretched state. Such a response is not only dictated by the entropic spring-like response of hydrophilic chains but also by the behavior of hydrophobic stretched chains in an aqueous environment. In the stretched state, the hydrophobic segments in contact with water, an unfavorable solvent, rapidly return to their original collapsed condition once the strain is removed. However, the enthalpic penalty is not significant, therefore, resilin is highly resilient. For our gels, we expect to see similar mechanical responses of the hydrophilic and hydrophobic segments mimicking the mechanical properties of resilin.
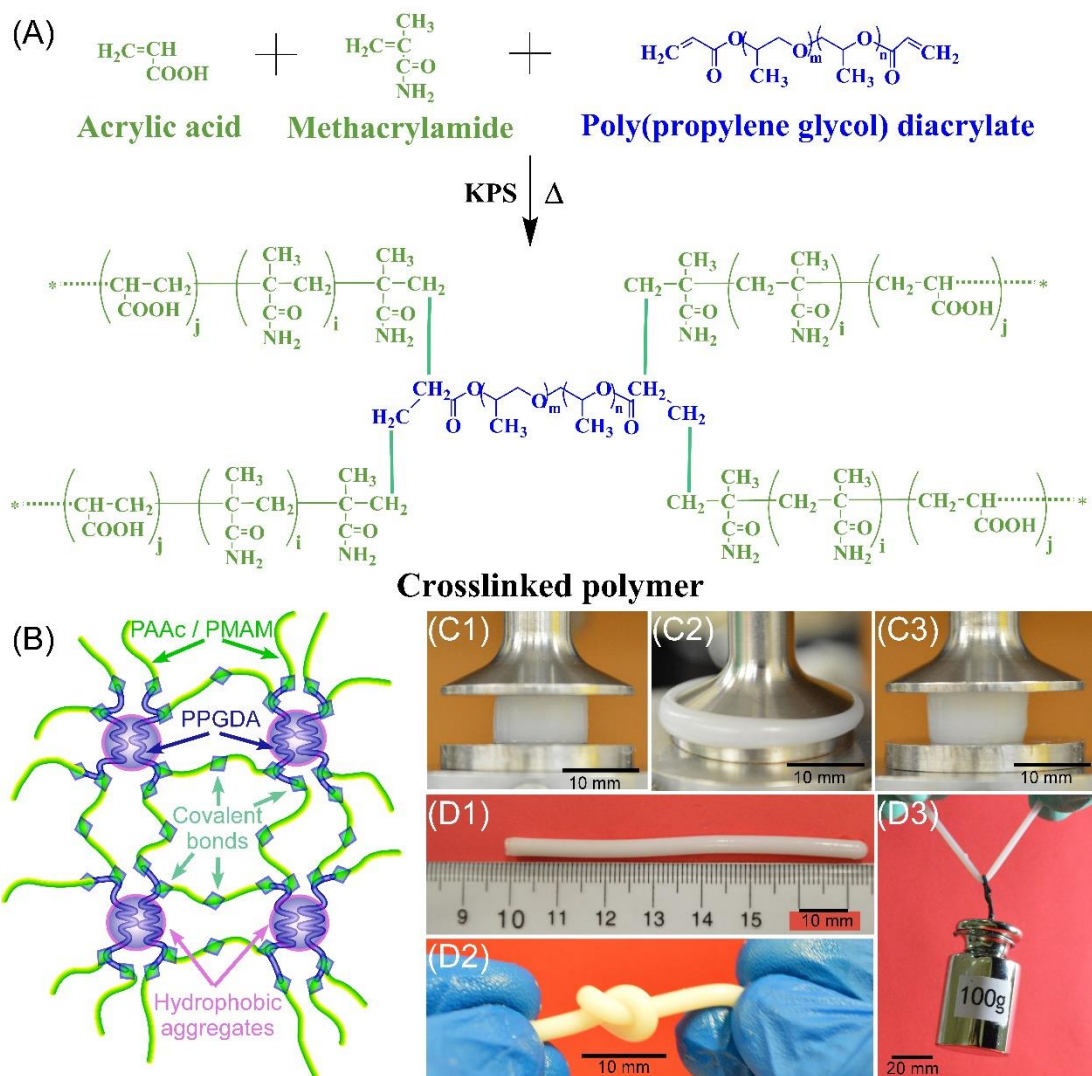
Figure 1. Chemical structure and stretchability of hydrogel. (A) Reaction scheme for the hydrogel formation. (B) The three-dimensional structure of hydrogel, where hydrophobic aggregates (pink spheres) containing PPGDA molecules (blue chains) are connected by the hydrophilic PAAc and PMAM chains (green chains). Here, the green diamonds represent covalent bonds. (C) Compression of a 27%-Gel sample representing the undeformed state (C1), after compression (C2), and after removing the stress (C3). (D) Complex deformation of a gel string (37%-Gel) in an undeformed state (D1), forming a knot (D2), and supporting 100 g deadweight (D3).

1   **Mechanical properties**

2   The synthesized gels are highly compressible and resilient. As displayed in Figure 1C, a

3   cylindrical sample with an initial height of 5 mm was compressed to 1 mm with a strain-rate of

4   0.2 s^{-1}, and the sample quickly recovered to the original height with a negligible residual strain

5   after the compressive strain was released. The sample has an ability to return to its original form

6   even after undergoing a complex deformation (Figure 1D1-2). The sample can also bear a

7   concentrated load without failing (Figure 1D3).

8   As the samples display excellent resilience behavior in compression mode, the stretchability and

9   gel modulus have been determined using tensile testing at room temperature (22 °C) utilizing a

10   custom-built instrument developed in our research group.[15,16] Figure 2A shows nominal stress

11   (σ) as a function of strain (ε) for 17%-, 27%-, and 37%-Gels obtained from these tensile

12   experiments using a strain-rate ($\dot{\varepsilon}$)≈0.048 s^{-1}. The σ was calculated considering the initial cross-

13   sectional area of the sample gauge region (see Figure S3). To determine the strain values

14   accurately, we have used an image analysis technique, where the distance between the lines drawn

15   on the sample as a function of time was used to estimate ε and $\dot{\varepsilon}$ (Figure 2B and Figure S3).[15,16]

16   This technique allows us to determine strain values more accurately in comparison to the

17   traditional methods, where the displacement of the sample clamp or a stage is tracked to determine

18   the strain values, possibly leading to an erroneous higher stretchability of the gel samples.[27] Our

19   gel samples display a typical s-shaped response of elastomers[12,28] and a high stretchability before

20   failing, ε_f (Figure 2C). For example, the ε_f for the 17%-Gel is as high as ≈8.6. Images of the

21   stretched gels with three different polymer concentrations are displayed in Figure S4A-C for

22   comparison. In addition, the experiments were also performed at $\dot{\varepsilon}$≈0.48 s^{-1}, however, no

1   noticeable change in the σ-ε behavior was observed by increasing $\dot{\varepsilon}$ an order of magnitude

2   (Figure S4D), indicating low energy dissipation in these gels.

3   The σ-ε responses display higher initial slopes with increasing polymer concentration,

4   indicating an increase in modulus. To determine the small-strain tensile modulus (E), the neo-

5   Hookean model expressed as $\sigma = (E/3)((\varepsilon+1)-(\varepsilon+1)^{-2})$ for the uniaxial loading was fitted over

6   the range of $0 \le \varepsilon \le 0.35$ (Figure S5).[28] The estimated E values are 15.1, 56.8, and 103.1 kPa for the

7   17%-, 27%-, and 37%-Gel, respectively (Figure 2D). These values are comparable to the other

8   crosslinked hydrogels like polyacrylamide,[29] hydrophobically modified acrylic gels,[22]

9   alginate/polyacrylamide,[30] or gelatin hydrogels.[31] With the increase in monomer concentration, a

10 higher modulus ($d\sigma/d\lambda$) can be noticed, however, the ε_f decreases with increasing monomer

11 concentration. The ε_f values of 27%-Gel and 37%-Gel are not significantly different, evaluated

12 using a t-test with 95% confidence interval. Note that these two gels display similar swelling

13 behavior. Also, the failure stress (σ_f) values of 17%- and 27%-Gels are not statistically different.

14 Since we have maintained a constant monomer to crosslinker ratio, an increase in monomer

15 concentration increases the crosslinking density leading to a higher gel modulus.[28] Strain-

16 stiffening behavior observed in all three gels at high ε can be related to the finite-extensibility of

17 the chains[32,33] as most likely, the hydrophobic aggregates dissociate, and the PPG chains are

18 stretched. Strain-stiffening allows these gels to carry a concentrated load, as seen in Figure 1D3,

19 despite not having a very high E.

20 In determining the resilience behavior of these gels, cyclic loading tests were performed on three

21 gel samples considered here. Although it is preferred to stretch the samples to a prescribed strain,

22 real-time strain measurements from the images have been found to be difficult. Therefore, the

1 samples were stretched to a prescribed stress value using $\dot{\varepsilon} \approx 0.048$ s^{-1} and then unloaded to zero

2 stress with the same $\dot{\varepsilon}$. After completion of one loading cycle, the stress was continuously

3 increased by 10 kPa for the next cycle until the sample failed, mostly at the ε_f values obtained

4 from the tensile tests (Figure 2C). Results for the 37%-Gel for particular stress values are shown

5 in Figure 2E-F. The loading and unloading cycles for all gels with 10 kPa step-increase are shown

6 in Figure S6, S7, and S8. The strain-recovery after unloading is almost complete, as the residual

7 strain has been found to be negligible, especially at the high-stretch values and for higher monomer

8 concentration. For example, the residual strain for all gel samples is $\approx 5.7\%$ for the $\sigma = 30$ kPa

9 cycle, however, it reduces to 2% for 37%-Gel for the $\sigma = 130$ kPa cycle. The actual strain-recovery

10 can be a little higher, particularly for the low applied stress, as we have a few percentages of

11 measurement error in capturing the position of marked lines (≈ 0.2 mm error in measuring distances

12 between the lines on the samples). The resilience behavior of these gels can be quantified as the

13 ratio of energy recovered during the unloading cycle to the energy absorbed during the loading

14 cycle. A remarkable resilience of $\approx 98\%$ is captured for 37%-Gel (Table S2). With a decrease in

15 the monomer concentration, the resilience reduces to 90.3% for 27%-Gel and 88.6% for 17%-Gel.

16 Overall, we have obtained less than 10% energy loss during a cycle, which is not very significant.

17   The high resilience of our gels can mostly be attributed to the reversible stretching of hydrophilic

18 chains. As discussed above, because of the presence of NaCl, the acid groups are mostly screened,

19 enhancing the stretchability of the chains.[21] When subjected to a load, the stretching of hydrophilic

20 chains between two crosslinks occurs, followed by the dissociation of hydrophobic aggregates and

21 subsequent stretching of hydrophobic blocks, as the entropic penalty in chain stretching is lower

22 than overcoming the hydrophobic association energy.[15,16] Once the load is removed, in addition to

23 the hydrophilic chains, the hydrophobic chains also retract quickly from the unfavorable aqueous

environment to form aggregates again, leading to high resilience and almost full strain recovery. The low hysteresis loop also indicates that the enthalpic loss associated with dissociation and reformation of hydrophobic aggregates is not significant, similar to that observed in the resilin. Therefore, the low molecular weight of the hydrophobic PPG-chains is beneficial.[10,34] In addition to the enthalpic contribution because of association and dissociation of hydrophobic blocks, the hysteresis in our gels can also be attributed to the viscous dissipation caused by the inhomogeneity and defects in the microstructure.

The resilience values of the present gels are comparable to those obtained for recombinant resilin and elastin with the resilience of $\approx 97\%$ and 90%, respectively.[1] The performance of our gels can also be compared with other synthetic hydrogels displaying high stretchability with low hysteresis. A majority of these systems is either polyethylene glycol (PEG) based hydrogels[9,35,36] or polymer-clay nanocomposite hydrogels.[10,34] The tetra-PEG systems display high stretchability and low hysteresis, however, their synthesis requires a relatively complex reaction route.[9,35] In comparison, PEG-based systems incorporated with hydrophobic polydimethylsiloxane blocks display relatively high modulus.[9] These systems display very high resilience ($\approx 98\%$), but the stretchability can be limited.[9] Polymer-clay nanocomposite hydrogels display high stretchability and low hysteresis over a limited range of strain, however, these gels can have a longer recovery time from the highly stretched state.[10,34] In contrast, our gels recover instantaneously, even at high strain. The instantaneous recovery of our samples was further explored through the retraction experiments.
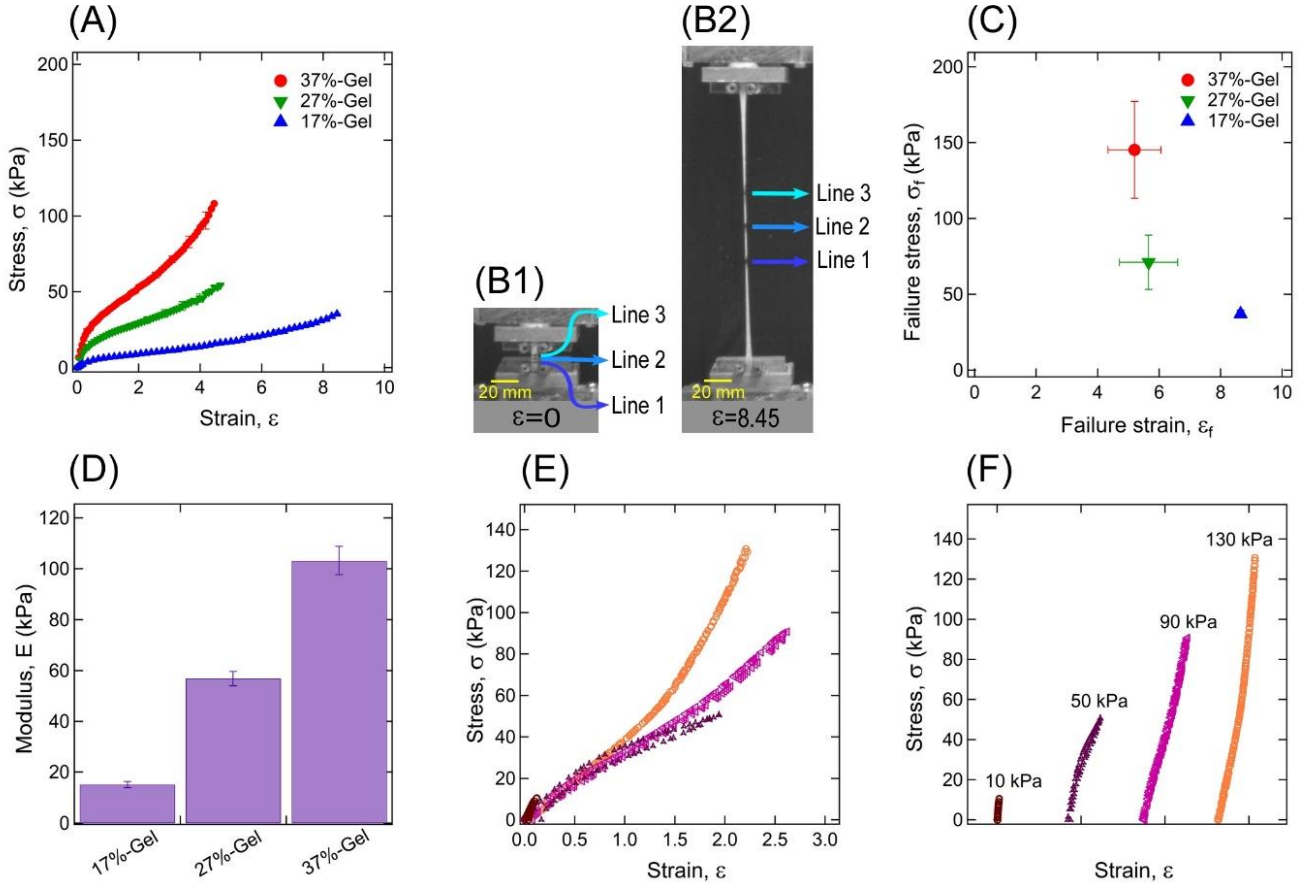
Figure 2. Tensile testing and cyclic loading experiments. (A) Nominal stress (σ) as a function of strain (ε) for 17%-, 27%-, and 37%-Gels. Results are an average of three runs with standard deviation. (B) Images of the 17%-Gel sample during a tensile experiment: (B1) initial condition ($\varepsilon = 0$), and (B2) before the failure of the gel, capturing high stretchability of the sample ($\varepsilon = 8.45$). (C) Failure stress (σ_f) and failure strain (ε_f) for the three gels. The error bars represent the standard deviation. (D) Young's modulus of the three gels obtained by fitting the neo-Hookean model to the experimental data up to $\varepsilon \approx 0.35$. The error bars represent the standard deviation. (E-F) Results from cyclic loading experiments for 37%-Gel plotted for the maximum stress values, $\sigma = 10, 30, 90,$ and 130 kPa. Each cycle is shifted by 0, 4, 8, and 12 units, respectively, along the strain-axis for clarity.

1   **Retractability of hydrogels.**

2   Figure 3 shows the results of retraction experiments performed on a 37%-Gel string using the

3   stretch ratio ($\lambda = \varepsilon + 1$) of 6. Here, the stretched string was cut at the bottom clamp using a pair of

4   scissors, and then the string was allowed to retract freely. The sample was marked with seven

5   equidistant lines (Figure 3A1-A2) to track the position of lines with time as the sample retracted.

6   The line positions were tracked from the release of the string until the time it slacked. The results

7   presented here correspond to Line 1, which achieved the highest velocity and acceleration during

8   the retraction. The position of Line 1 for all three gels are plotted as a function of time in Figure

9   3B for λ =6. The response of Line 1 can be divided into three regions. First, the initial plateau for

10   a few milliseconds (ms) indicating that the string is still in the static condition. Next, as time

11   progresses, the sample starts to retract. It accelerates from the static condition to the peak velocity

12   resulting in curvature in the position vs. time data.[8,37–41] A sharper curvature signifies a higher

13   acceleration value. Finally, the string reaches a constant velocity displayed by a straight line with

14   a constant slope.

15   The line position with time was fitted with a fifth-order Fourier series (Figure S9), and the

16   obtained function was then differentiated for estimating velocity and acceleration (see Supporting

17   Information). The estimated velocity values for the three gels are shown in Figure 3C, capturing

18   static condition, acceleration, and constant velocity. The estimated acceleration values are shown

19   in Figure 3D representing the peak values corresponding to the curvature in the position-time plot.

20   Note that other functions, such as cubic spline, can be used to fit the experimental data, but we

21   found that Fourier series with sufficient number of coefficients (5th order considered here) and

22   with an appropriate value of ω, the data can be fitted reasonably well. Figure 3E and F summarize

23   the maximum velocity and acceleration for the λ values of 3-6. With the increase in monomer

1   concentration, both velocity and acceleration increase suggesting that higher values can be

2   obtained by further increasing the monomer concentration or partially drying the samples. The

3   maximum velocity and acceleration for 37%-Gel and $\lambda =6$ are ≈16 m s^{-1} and $\approx4\times10^3$ m s^{-2},

4   respectively.

5   The retraction velocity values are comparable to those of a frog jump (≈4.5 m s^{-1}), froghopper

6   jump (≈4.7 m s^{-1}), and Mantis shrimp appendage strike (≈30 m s^{-1}).[5] The acceleration is similar to

7   the jump of a froghopper ($\approx5.4\times10^3$ m s^{-2}).[5] The retraction velocity in our gel is lower than dry,

8   vulcanized natural rubber (≈125 m s^{-1})[37] but somewhat similar to the polyurethane elastomers (≈25

9   m s^{-1}).[5] To the best of our knowledge, this is the first demonstration of achieving such a high

10   velocity and acceleration in hydrogels.

11   The retraction mechanism in elastomers has been previously studied in detail using a very similar

12   experimental protocol described above.[8,37–40] A sudden release of the lower end of a sample from

13   a stretched state causes the propagation of a retraction pulse or stress wave with a velocity v in the

14   longitudinal direction.[37,39,40] Note that the Line 1 velocity (u) is different and is lower than v, as u

15   originates from the momentum generated by the retraction pulse. It can be shown that

16   $u=\sqrt{\dfrac{\sigma(\lambda-1)}{\rho}}$ and $v=\lambda\sqrt{\dfrac{\sigma}{\rho(\lambda-1)}}$ from momentum balance.[37] Here, λ is the stretch ratio from

17   which the sample is released, and σ is the corresponding stress value, and ρ is the density of the

18   system. Note that for linear elastic material with a modulus E, $u=(\lambda-1)\sqrt{E/\rho}$, and $v=\lambda\sqrt{E/\rho}$

19   , as reported in the literature.[38,39] These relationships corresponding to linear elastic materials are

20   not suitable for our case as the modulus of our system is changing with applied stretch (Figure

21   2A). Note that in isotropic media, the sound velocity can be estimated as $\sqrt{K/\rho}$, independent of

22   λ, where K is the bulk modulus of the material.[40] In the retraction experiments, the retraction

1 pulse is dictated by the E values, therefore, u and v values are typically a couple of orders of

2 magnitude lower than the sound velocity in elastomers.[39]

3   The free retraction velocity of our sample was then compared with the theoretically estimated u

4 value, $u = \sqrt{\sigma(\lambda - 1)/\rho}$.[39,41,37] We have used density, $\rho \approx 1.05$, 1.10, and 1.14 g mL^{-1} for 17%-,

5 27%-, and 37%-Gel, respectively. σ corresponding to a particular λ was estimated from Figure

6 2A. The density of each gel was determined by measuring the mass of the as-prepared cubic-

7 shaped sample and the volume occupied by that sample. Figure 3E compares u as a function of λ

8 with the experimentally obtained values of Line 1 for each gel.

9   Here, the predicted u values are 1.1-1.7 times higher than the experimentally obtained retraction

10 velocity of Line 1 but are of the same order of magnitude. The equation used for estimating u

11 originates from the momentum balance, therefore, it does not account for any dissipation in the

12 system. The lower retraction velocity in our system than that predicted theoretically can be related

13 to the viscous dissipation that can arise because of the presence of defects in the gel microstructure.

14 For the higher polymer concentration, an increase in the number of defects can be anticipated,

15 resulting in a higher deviation from the theoretical prediction. The cyclic loading experiments

16 show a very small amount of hysteresis or dissipation, interestingly, that small dissipation may

17 have caused the reduction in retraction velocity from the theoretical prediction for a perfectly

18 elastic material. This dissipation is also likely to lower the acceleration values in our gels compared

19 to that observed in some biological systems $\approx 10^5$ m s^{-2}.[5]
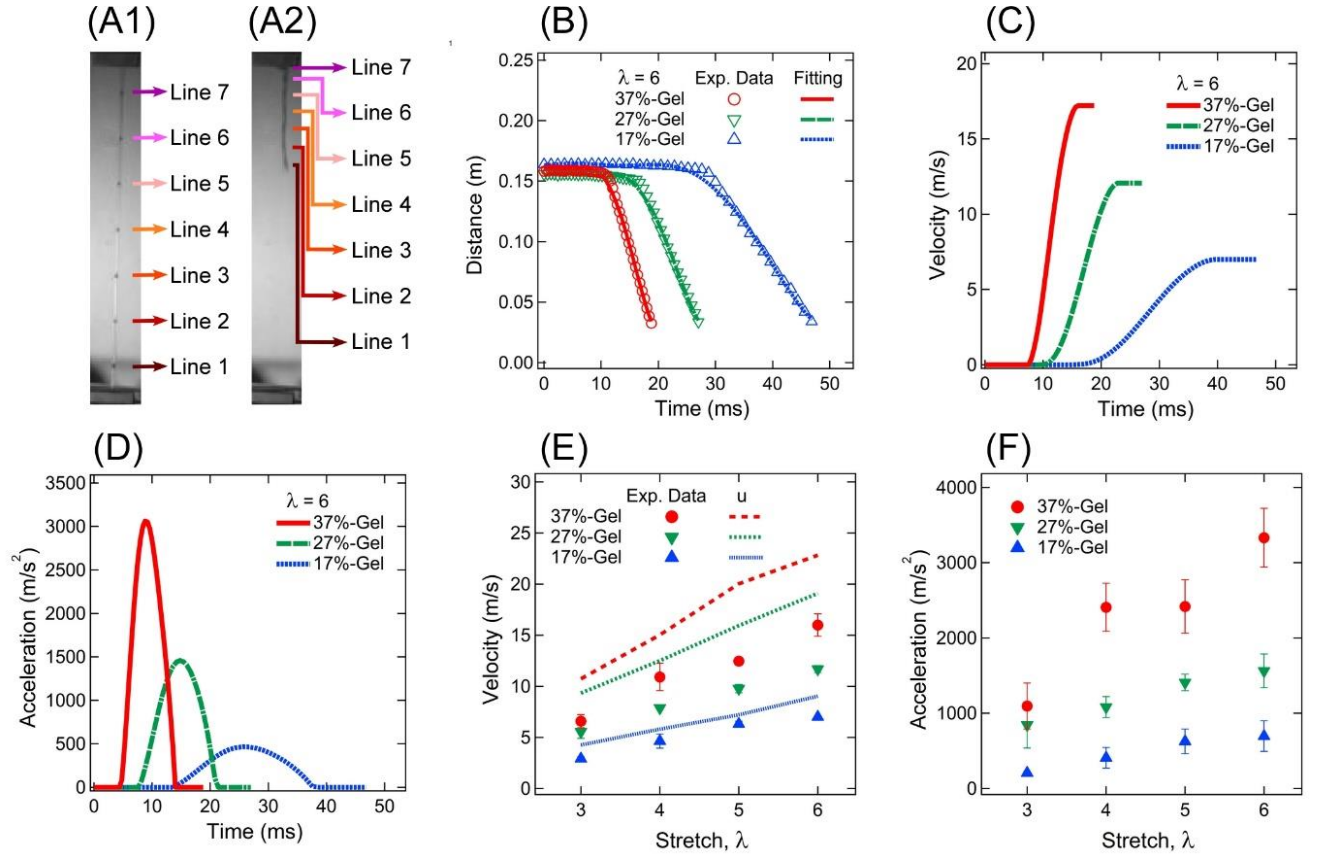
20

21

22

Figure 3. Retraction of gel samples from a stretched-state. Image of a 37%-Gel string: (A1) at the stretched condition, λ =6 at t=0 ms., marked with 7 lines (Line 1-7), and (A2) fully retracted after $t \approx$ 19 ms. (B) Position, (C) velocity, and (D) acceleration of Line 1 as a function of time for all gels with λ =6. In (B) both the experimental data and the fitting of the Fourier series are shown. (E) Retraction velocity as a function of different λ for all three gels. A comparison of the experimentally observed velocity of Line 1 with theoretically predicted retraction velocity (u) as a function of λ. (F) Maximum acceleration corresponding to Line 1 as a function of λ for all three gels. The error bars represent the standard deviation.

Solid projectile launching by hydrogels. Since our gels have high stretchability and resilience, we have shown their applications for catapulting solid projectiles. As shown in Figure 4, by using a 37%-Gel string, we have been able to launch a solid projectile of 1.53 g to a distance (L) of 7.96±0.24 m. The achieved projectile velocity was 15.93±0.63 m s^{-1}, and 93% of the energy stored in the system during stretching was converted into kinetic energy. This was achieved for $\lambda \approx 6$, and different L values can be obtained by considering the different λ values. Also, the sample can be reused multiple times. This further opens up novel applications of the gels reported here.
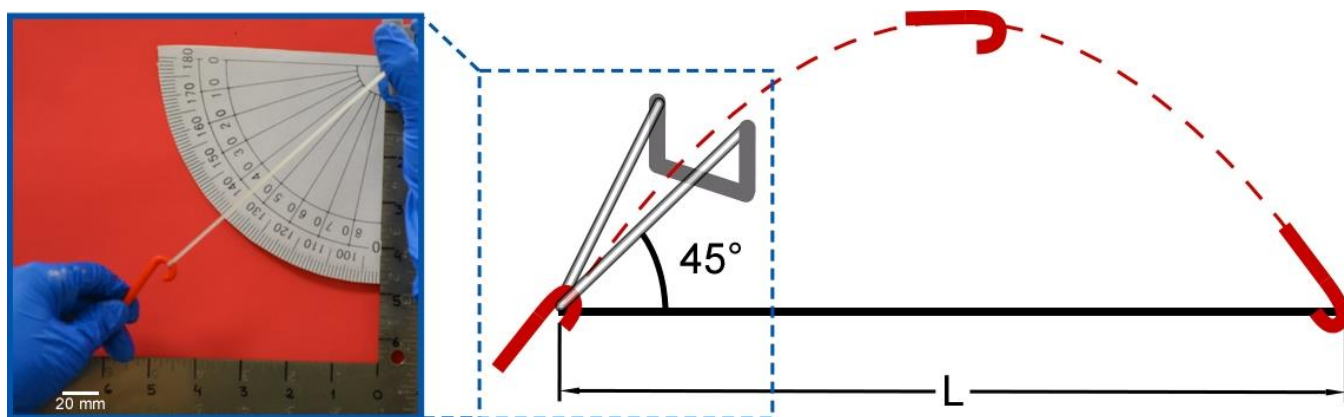
Figure 4. Application of gels for launching a projectile. Image and scheme of a projectile launching by using a 37%-Gel for stretch, $\lambda = 6$.

Conclusions

In conclusion, we report a novel hydrogel synthesized through a simple free radical copolymerization scheme. By selecting an appropriate ratio of hydrophilic PAAc and PMAM chains and hydrophobic associations of PPGDA chains, highly stretchable ($\lambda \approx 8.6$) and resilient gels (≈98%) with a negligible residual strain (≈2%) have been obtained. After released from a

1 stretched state, the gel samples achieve retraction velocity, as high as ≈ 16 m s^{-1} and acceleration

2 $\approx 4 \times 10^3$ m s^{-2}. These properties resemble naturally occurring elastomeric biopolymers, like resilin.

3 High resilience and stretchability can be utilized in many activities, such as catapulting a projectile

4 or other power amplification systems. Because of a simple synthetic route, the hydrogel properties

5 can be further tuned, and new applications can be envisioned. Further, based on the results

6 presented here, we can hypothesize that the design of materials aimed for power amplified

7 activities requires (1) high modulus to density ratio, (2) high stretchability, and (3) minimal energy

8 dissipation or high energy recovery.

9

10 ASSOCIATED CONTENT

11 **Supporting Information:** Fourier transform infrared spectroscopy of monomers and gel;

12 Images of swelling behavior of gels; Scheme and images of the dimensions of dogbone samples

13 with marked-lines; Images and data of gel stretchability and strain-rate dependence; Graph

14 corresponding to the determination of the tensile modulus of gels; cyclic loading curves of 17%-,

15 27%-, and 37%-Gels; Graph corresponding to the marked-line positions as a function of time

16 during retraction and fitted parameters corresponding to Line 1 for 37%-Gel at stretch of 6. Tables

17 of the results of swelling behavior and resilience of gels.

18

19 **AUTHOR INFORMATION**

20 Corresponding Author

21 *Santanu Kundu. E-mail: santanukundu@che.msstate.edu

22

Author contributions

S.K. proposed and supervised this project. S.K., R.M.B.P., and S.M. analyzed the data and wrote the paper. R.M.B.P., S.M., and B.M. performed the experiments. R.W. and S.M.H. conducted preliminary experiments. All authors have given approval to the final version of the manuscript.

REFERENCES

(1)   Elvin, C. M.; Carr, A. G.; Huson, M. G.; Maxwell, J. M.; Pearson, R. D.; Vuocolo, T.; Liyou, N. E.; Wong, D. C. C.; Merritt, D. J.; Dixon, N. E. Synthesis and Properties of Crosslinked Recombinant Pro-Resilin. *Nature* **2005**, *437* (7061), 999–1002. https://doi.org/10.1038/nature04085.

(2)   Nairn, K. M.; Lyons, R. E.; Mulder, R. J.; Mudie, S. T.; Cookson, D. J.; Lesieur, E.; Kim, M.; Lau, D.; Scholes, F. H.; Elvin, C. M. A Synthetic Resilin Is Largely Unstructured. *Biophys. J.* **2008**, *95* (7), 3358–3365. https://doi.org/10.1529/biophysj.107.119107.

(3)   Qin, G.; Hu, X.; Cebe, P.; Kaplan, D. L. Mechanism of Resilin Elasticity. *Nat. Commun.* **2012**, *3* (1), 1003. https://doi.org/10.1038/ncomms2004.

(4)   Su, R. S.-C.; Kim, Y.; Liu, J. C. Resilin: Protein-Based Elastomeric Biomaterials. *Acta Biomater.* **2014**, *10* (4), 1601–1611. https://doi.org/10.1016/j.actbio.2013.06.038.

1   (5)   Ilton, M.; Bhamla, M. S.; Ma, X.; Cox, S. M.; Fitchett, L. L.; Kim, Y.; Koh, J.;

2   Krishnamurthy, D.; Kuo, C.-Y.; Temel, F. Z.; Crosby, A. J.; Prakash, M.; Sutton, G. P.;

3   Wood, R. J.; Azizi, E.; Bergbreiter, S.; Patek, S. N. The Principles of Cascading Power

4   Limits in Small, Fast Biological and Engineered Systems. *Science (80-.).* **2018**, *360* (6387),

5   eaao1082. https://doi.org/10.1126/science.aao1082.

6   (6)   Patek, S. N.; Korff, W. L.; Caldwell, R. L. Deadly Strike Mechanism of a Mantis Shrimp.

7   *Nature* **2004**, *428* (6985), 819–820. https://doi.org/10.1038/428819a.

8   (7)   Gosline, J.; Lillie, M.; Carrington, E.; Guerette, P.; Ortlepp, C.; Savage, K. Elastic Proteins:

9   Biological Roles and Mechanical Properties. *Philos. Trans. R. Soc. London. Ser. B Biol.*

10   *Sci.* **2002**, *357* (1418), 121–132. https://doi.org/10.1098/rstb.2001.1022.

11 (8)   Ilton, M.; Cox, S. M.; Egelmeers, T.; Sutton, G. P.; Patek, S. N.; Crosby, A. J. The Effect

12   of Size-Scale on the Kinematics of Elastic Energy Release. *Soft Matter* **2019**, *15* (46), 9579–

13   9586. https://doi.org/10.1039/C9SM00870E.

14 (9)   Cui, J.; Lackey, M. A.; Madkour, A. E.; Saffer, E. M.; Griffin, D. M.; Bhatia, S. R.; Crosby,

15   A. J.; Tew, G. N. Synthetically Simple, Highly Resilient Hydrogels. *Biomacromolecules*

16   **2012**, *13* (3), 584–588. https://doi.org/10.1021/bm300015s.

17 (10) Su, X.; Mahalingam, S.; Edirisinghe, M.; Chen, B. Highly Stretchable and Highly Resilient

18   Polymer-Clay Nanocomposite Hydrogels with Low Hysteresis. *ACS Appl. Mater.*

19   *Interfaces* **2017**, *9* (27), 22223–22234. https://doi.org/10.1021/acsami.7b05261.

20 (11) Tjin, M. S.; Low, P.; Fong, E. Recombinant Elastomeric Protein Biopolymers: Progress and

21   Prospects. *Polym. J.* **2014**, *46* (8), 444–451. https://doi.org/10.1038/pj.2014.65.

1   (12) Sun, T. L.; Kurokawa, T.; Kuroda, S.; Ihsan, A. Bin; Akasaki, T.; Sato, K.; Haque, M. A.;

2   Nakajima, T.; Gong, J. P. Physical Hydrogels Composed of Polyampholytes Demonstrate

3   High Toughness and Viscoelasticity. *Nat. Mater.* **2013**, *12* (10), 932–937.

4   https://doi.org/10.1038/nmat3713.

5   (13) Gao, G.; Du, G.; Sun, Y.; Fu, J. Self-Healable, Tough, and Ultrastretchable Nanocomposite

6   Hydrogels Based on Reversible Polyacrylamide/Montmorillonite Adsorption. *ACS Appl.*

7   *Mater. Interfaces* **2015**, *7* (8), 5029–5037. https://doi.org/10.1021/acsami.5b00704.

8   (14) Xiang, S.; Li, T.; Dong, W.; Lu, Q. A Facile Method to Fabricate Tough Hydrogel with

9   Ultra-Wide Adjustable Stiffness, Stress, and Fast Recoverability. *J. Polym. Sci. Part B*

10   *Polym. Phys.* **2018**, *56* (21), 1469–1474. https://doi.org/10.1002/polb.24737.

11 (15) Mishra, S.; Badani Prado, R. M.; Lacy, T. E.; Kundu, S. Investigation of Failure Behavior

12   of a Thermoplastic Elastomer Gel. *Soft Matter* **2018**, *14* (39), 7958–7969.

13   https://doi.org/10.1039/C8SM01397G.

14 (16) Mishra, S.; Badani Prado, R. M.; Zhang, S.; Lacy, T. E.; Gu, X.; Kundu, S. Mechanical

15   Properties and Failure Behavior of Physically Assembled Triblock Copolymer Gels with

16   Varying Midblock Length. *J. Polym. Sci. Part B Polym. Phys.* **2019**, *57* (15), 1014–1026.

17   https://doi.org/10.1002/polb.24860.

18 (17) Sammalkorpi, M.; Karttunen, M.; Haataja, M. Ionic Surfactant Aggregates in Saline

19   Solutions: Sodium Dodecyl Sulfate (SDS) in the Presence of Excess Sodium Chloride

20   (NaCl) or Calcium Chloride (CaCl 2). *J. Phys. Chem. B* **2009**, *113* (17), 5863–5870.

21   https://doi.org/10.1021/jp901228v.

1   (18)   Hooper, H. H.; Baker, J. P.; Blanch, H. W.; Prausnitz, J. M. Swelling Equilibria for

2   Positively Ionized Polyacrylamide Hydrogels. *Macromolecules* **1990**, *23* (4), 1096–1104.

3   https://doi.org/10.1021/ma00206a031.

4   (19)   Yang, M.; Liu, C.; Li, Z.; Gao, G.; Liu, F. Temperature-Responsive Properties of

5   Poly(Acrylic Acid-Co-Acrylamide) Hydrophobic Association Hydrogels with High

6   Mechanical Strength. *Macromolecules* **2010**, *43* (24), 10645–10651.

7   https://doi.org/10.1021/ma1022555.

8   (20)   Zhang, F.; Guo, Z.; Gao, H.; Li, Y.; Ren, L.; Shi, L.; Wang, L. Synthesis and Properties of

9   Sepiolite/Poly (Acrylic Acid-Co-Acrylamide) Nanocomposites. *Polym. Bull.* **2005**, *55* (6),

10   419–428. https://doi.org/10.1007/s00289-005-0458-2.

11 (21)   Walker, A.; Vratsanos, M.; Kozawa, S.; Askew, T.; Hemmendinger, K.; McGrail, B.;

12   Bedford, N.; Wnek, G. Enhanced Elasticity in Poly(Acrylic Acid) Gels via Synthesis in the

13   Presence of High Concentrations of Select Salts. *Soft Matter* **2019**, *15* (38), 7596–7604.

14   https://doi.org/10.1039/C9SM01101C.

15 (22)   Miquelard-Garnier, G.; Hourdet, D.; Creton, C. Large Strain Behaviour of Nanostructured

16   Polyelectrolyte Hydrogels. *Polymer (Guildf).* **2009**, *50* (2), 481–490.

17   https://doi.org/10.1016/j.polymer.2008.11.045.

18 (23)   Liu, X.; Duan, L.; Gao, G. Rapidly Self-Recoverable and Fatigue-Resistant Hydrogels

19   Toughened by Chemical Crosslinking and Hydrophobic Association. *Eur. Polym. J.* **2017**,

20   *89* (October 2016), 185–194. https://doi.org/10.1016/j.eurpolymj.2017.02.025.

21 (24)   Alexandridis, P.; Alan Hatton, T. Poly(Ethylene Oxide)-Poly(Propylene Oxide)-

Poly(Ethylene Oxide) Block Copolymer Surfactants in Aqueous Solutions and at Interfaces: Thermodynamics, Structure, Dynamics, and Modeling. *Colloids Surfaces A Physicochem. Eng. Asp.* **1995**, *96* (1–2), 1–46. https://doi.org/10.1016/0927-7757(94)03028-X.

(25) Dubey, S.; Bajpai, S. K. Poly(Methacrylamide-Co-Acrylic Acid) Hydrogels for Gastrointestinal Delivery of Theophylline. I. Swelling Characterization. *J. Appl. Polym. Sci.* **2006**, *101* (5), 2995–3008. https://doi.org/10.1002/app.23542.

(26) Baker, J. P.; Stephens, D. R.; Blanch, H. W.; Prausnitz, J. M. Swelling Equilibria for Acrylamide-Based Polyampholyte Hydrogels. *Macromolecules* **1992**, *25* (7), 1955–1958. https://doi.org/10.1021/ma00033a019.

(27) Mrozek, R. A.; Leighliter, B.; Gold, C. S.; Beringer, I. R.; Yu, J. H.; VanLandingham, M. R.; Moy, P.; Foster, M. H.; Lenhart, J. L. The Relationship between Mechanical Properties and Ballistic Penetration Depth in a Viscoelastic Gel. *J. Mech. Behav. Biomed. Mater.* **2015**, *44*, 109–120. https://doi.org/10.1016/j.jmbbm.2015.01.001.

(28) Treloar, L. R. G. *The Physics of Rubber Elasticity*; Oxford University Press, USA, 1975.

(29) Kundu, S.; Crosby, A. J. Cavitation and Fracture Behavior of Polyacrylamide Hydrogels. *Soft Matter* **2009**, *5* (20), 3963. https://doi.org/10.1039/b909237d.

(30) Sun, J.-Y.; Zhao, X.; Illeperuma, W. R. K.; Chaudhuri, O.; Oh, K. H.; Mooney, D. J.; Vlassak, J. J.; Suo, Z. Highly Stretchable and Tough Hydrogels. *Nature* **2012**, *489* (7414), 133–136. https://doi.org/10.1038/nature11409.

(31) Frieberg, B. R.; Garatsa, R.-S.; Jones, R. L.; Bachert, J. O.; Crawshaw, B.; Liu, X. M.; Chan, E. P. Viscoplastic Fracture Transition of a Biopolymer Gel. *Soft Matter* **2018**, *14* (23),

4696–4701. https://doi.org/10.1039/C8SM00722E.

(32) Hashemnejad, S. M.; Kundu, S. Nonlinear Elasticity and Cavitation of a Triblock Copolymer Gel. *Soft Matter* **2015**, *11* (21), 4315–4325. https://doi.org/10.1039/C5SM00330J.

(33) Erk, K. A.; Henderson, K. J.; Shull, K. R. Strain Stiffening in Synthetic and Biopolymer Networks. *Biomacromolecules* **2010**, *11* (5), 1358–1363. https://doi.org/10.1021/bm100136y.

(34) Zhu, M.; Liu, Y.; Sun, B.; Zhang, W.; Liu, X.; Yu, H.; Zhang, Y.; Kuckling, D.; Adler, H.-J. P. A Novel Highly Resilient Nanocomposite Hydrogel with Low Hysteresis and Ultrahigh Elongation. *Macromol. Rapid Commun.* **2006**, *27* (13), 1023–1028. https://doi.org/10.1002/marc.200600159.

(35) Kamata, H.; Akagi, Y.; Kayasuga-Kariya, Y.; Chung, U. -i.; Sakai, T. "Nonswellable" Hydrogel Without Mechanical Hysteresis. *Science (80-.).* **2014**, *343* (6173), 873–875. https://doi.org/10.1126/science.1247811.

(36) Sakai, T.; Akagi, Y.; Matsunaga, T.; Kurakazu, M.; Chung, U.; Shibayama, M. Highly Elastic and Deformable Hydrogel Formed from Tetra-Arm Polymers. *Macromol. Rapid Commun.* **2010**, *31* (22), 1954–1959. https://doi.org/10.1002/marc.201000286.

(37) Tunnicliffe, L. B.; Thomas, A. G.; Busfield, J. J. C. The Free Retraction of Natural Rubber: A Momentum-Based Model. *Polym. Test.* **2015**, *47*, 36–41. https://doi.org/10.1016/j.polymertesting.2015.07.012.

(38) James, H. M.; Guth, E. Theory of the Retraction of Stressed Rubber. *Phys. Rev.* **1944**, *66*
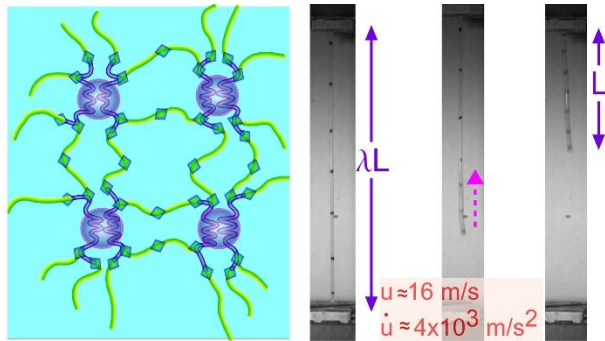
1   (1–2), 33–33. https://doi.org/10.1103/PhysRev.66.33.

2 (39) Gent, A. N.; Marteny, P. The Effect of Strain upon the Velocity of Sound and the Velocity

3   of Free Retraction for Natural Rubber. *J. Appl. Phys.* **1982**, *53* (9), 6069–6075.

4   https://doi.org/10.1063/1.331558.

5 (40) Bogoslovov, R. B.; Roland, C. M. Viscoelastic Effects on the Free Retraction of Rubber. *J.*

6   *Appl. Phys.* **2007**, *102* (6), 063531. https://doi.org/10.1063/1.2784018.

7 (41) Mason, P.; A, P. R. S. L. Finite Elastic Wave Propagation in Rubber. *Proc. R. Soc. London.*

8   *Ser. A. Math. Phys. Sci.* **1963**, *272* (1350), 315–330.

9   https://doi.org/10.1098/rspa.1963.0056.

10

11

12

13

14

15

16

17

18

19

Table of Contents (TOC) graphic

λL

u ≈ 16 m/s

$\dot{u}$ ≈ 4x10^3 m/s^2

L

Supporting Information

Achieving high-speed retraction in a stretchable hydrogel

Rosa Maria Badani Prado, Satish Mishra, Buckston Morgan, Rangana Wijayapala,

Seyed Meysam Hashemnejad, Santanu Kundu*

Dave C. Swalm School of Chemical Engineering, 323 Presidents Circle, Mississippi State

University, MS State, MS 39762, USA.

Corresponding Author

*Santanu Kundu. E-mail: santanukundu@che.msstate.edu
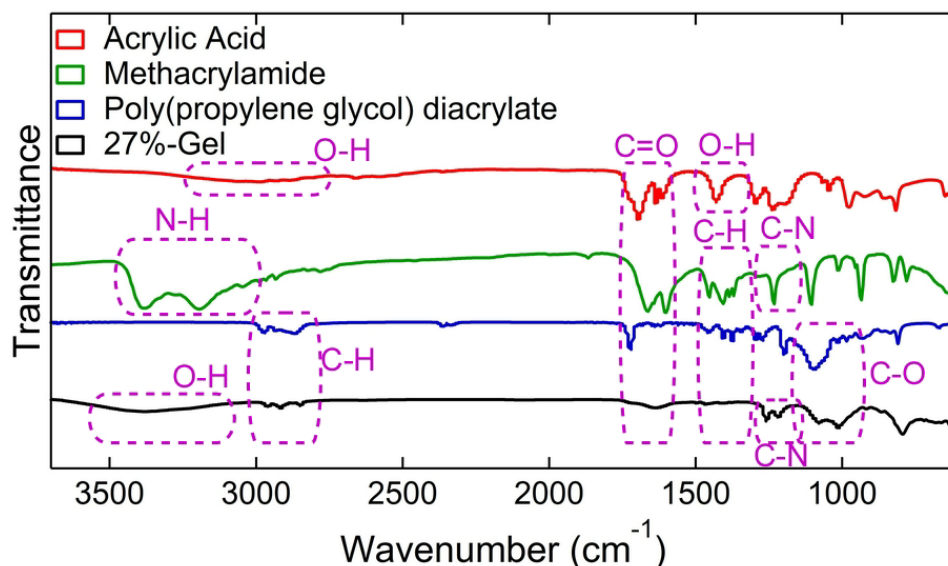
Figure S1. FTIR spectrum of acrylic acid, methacrylamide, poly(propylene glycol) diacrylate, and 27%-Gel.

The spectrum of acrylic acid (AAc) displays a broad band at $\approx$2988 cm^{-1} attributed to the O-H stretching, a peak at $\approx$1431 cm^{-1} corresponding to O-H bending, and a peak at $\approx$1695 cm^{-1} for C=O stretching, all related to the carboxyl groups.[1] Methacrylamide (MAM) spectrum displays peaks for the amide group at $\approx$2195 cm^{-1} and 3385 cm^{-1} attributed to the N-H stretching along with a peak at $\approx$1660 cm^{-1} for the C=O stretching and at $\approx$1230 cm^{-1} for the C-N stretching.[2] It also has peaks at $\approx$1400 and 1450 cm^{-1} attributed to the C-H bending. Poly(propylene glycol) diacrylate (PPGDA) spectrum displays peaks at $\approx$2869 and 2971 cm^{-1} attributed to the C-H stretching, at $\approx$1374 and 1405 cm^{-1} attributed to the C-H bending, at $\approx$1722 cm^{-1} for C=O stretching, and at $\approx$1096 cm^{-1} for the C-O stretching.[3] The crosslinking and polymerization of the compounds can be understood from the spectrum[1,2] of 27%-Gel, where (1) a broad band is shown at $\approx$3375 cm^{-1} attributed to O-H stretching likely overlapped with N-H stretching, both related to the AAc, MAM, and PPGDA interaction, (2) peaks at $\approx$2849 and 2961 cm^{-1} attributed to the C-H stretching related

to the presence of PPGDA in the structure, (3) a peak of low intensity at $\approx$1635 cm^{-1} related to C=O stretching coming from the presence of all the compounds, (4) a peak with low intensity at $\approx$1467 cm^{-1} attributed to the C-H bending likely related to the crosslinking of the compounds, (5) peaks at $\approx$1219 cm^{-1} and 1258 cm^{-1} for C-N stretching possibly related to the crosslinked MAM, (6) and a peak at $\approx$1080 cm^{-1} for the C-O stretching related to the presence of PPGDA.
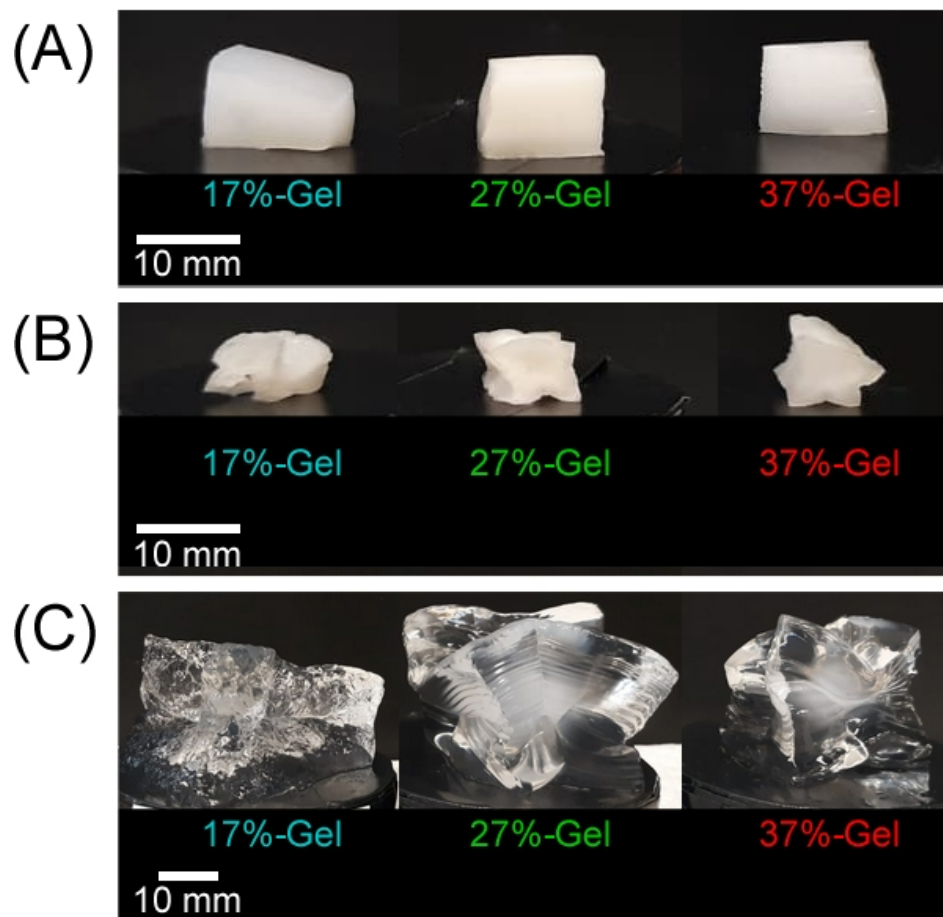
Figure S2. Swelling behavior of gels. (A) As-prepared 17%-, 27%-, and 37%-Gels. (B) Dried gels after 72 h of drying. (C) Gels after swelling for 24 h.
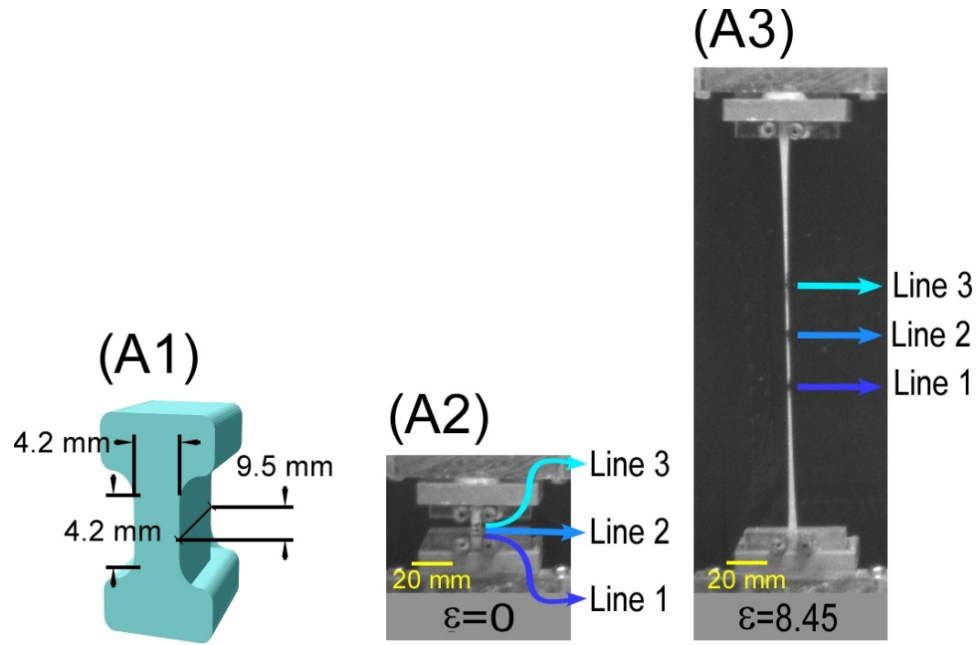
Figure S3. Dimensions of dogbone samples with marked-lines. (A1) Schematic of the dogbone-shape specimen for tensile experiments representing the dimensions. Images of tensile testing indicating the marked lines on the sample (17%-Gel) that were used to measure the strain (ε) and strain-rate ($\dot{\varepsilon}$). (A2) Unstretched sample, ε=0, and (A3) stretched sample, ε=8.45.
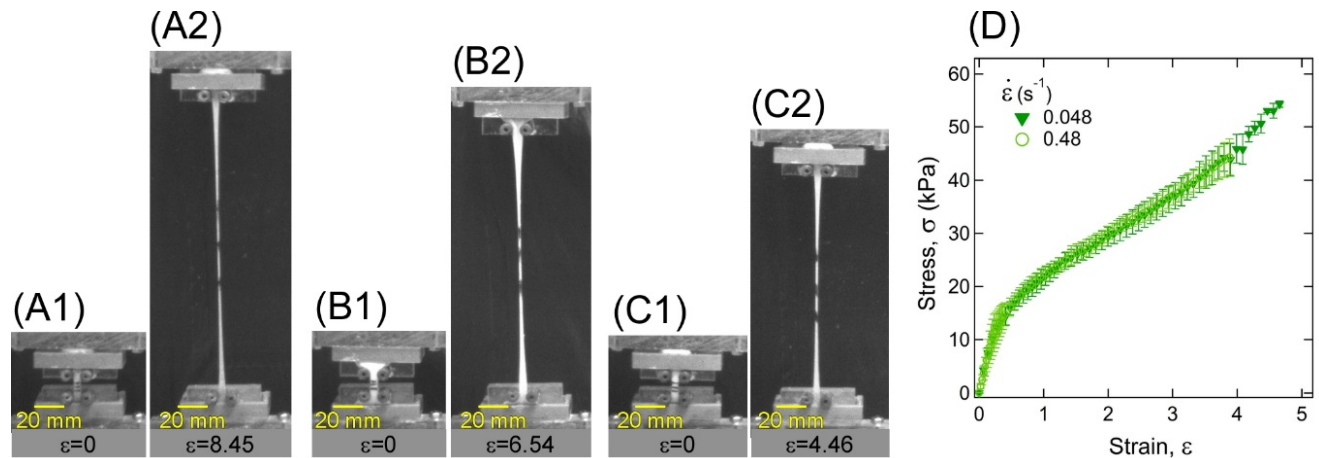
Figure S4. Gel stretchability and strain-rate dependence. Images of a 17%-Gel at the unstretched condition (ε =0) (A1) and the maximum stretched condition (ε =8.45) (A2). Images of 27%-Gel at the unstretched condition (ε =0) (B1), and the maximum stretched condition (ε =6.54) (B2). Images of 37%-Gel at the unstretched condition (ε =0) (C1), and the maximum stretched condition (ε =4.46) (C2). (D) Nominal stress (σ) as a function of strain (ε) for a 27%-Gel obtained from tensile testing experiments at strain-rate ($\dot{\varepsilon}$) 0.048 s^{-1} (dark green triangles) and 0.48 s^{-1} (light green open circles). The error bars represent the standard deviation.
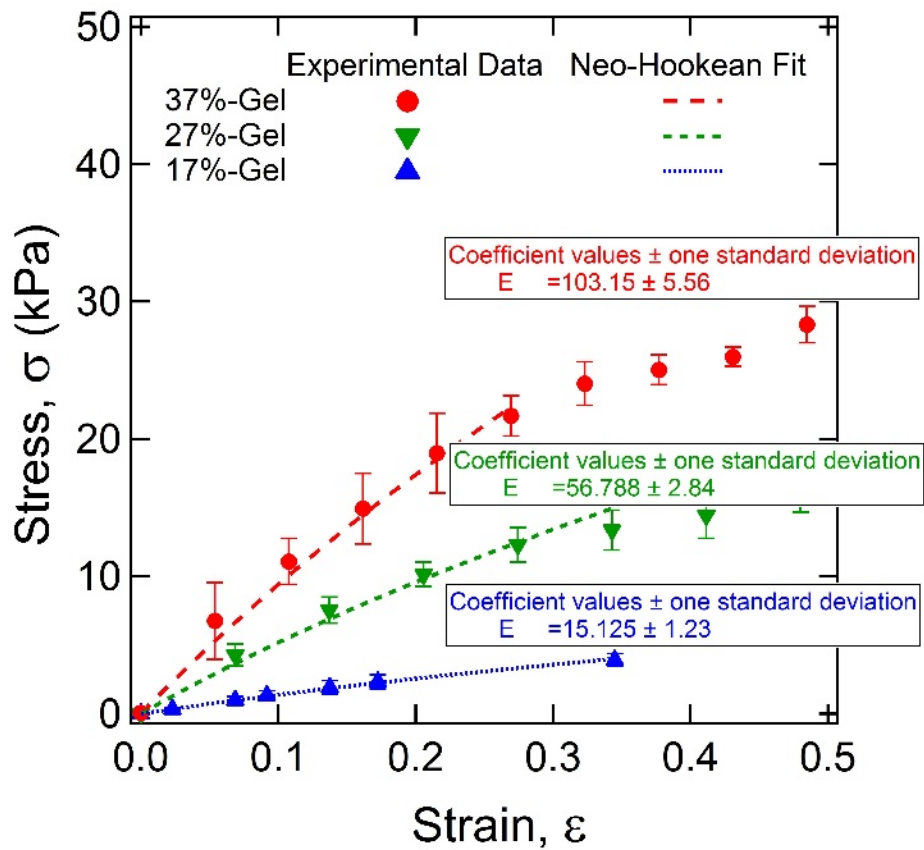
Figure S5. Tensile modulus of gels. Nominal stress (σ) as a function of strain ($0 \leq \varepsilon \leq 0.35$) for 17%-, 27%-, and 37%-Gels fitted with the neo-Hookean model for uniaxial loading. The corresponding tensile modulus (E) values for 17%-, 27%-, and 37%-Gels have been estimated as $\approx$15.1, 56.8, and 103.1 kPa, respectively. The error bars represent the standard deviation.
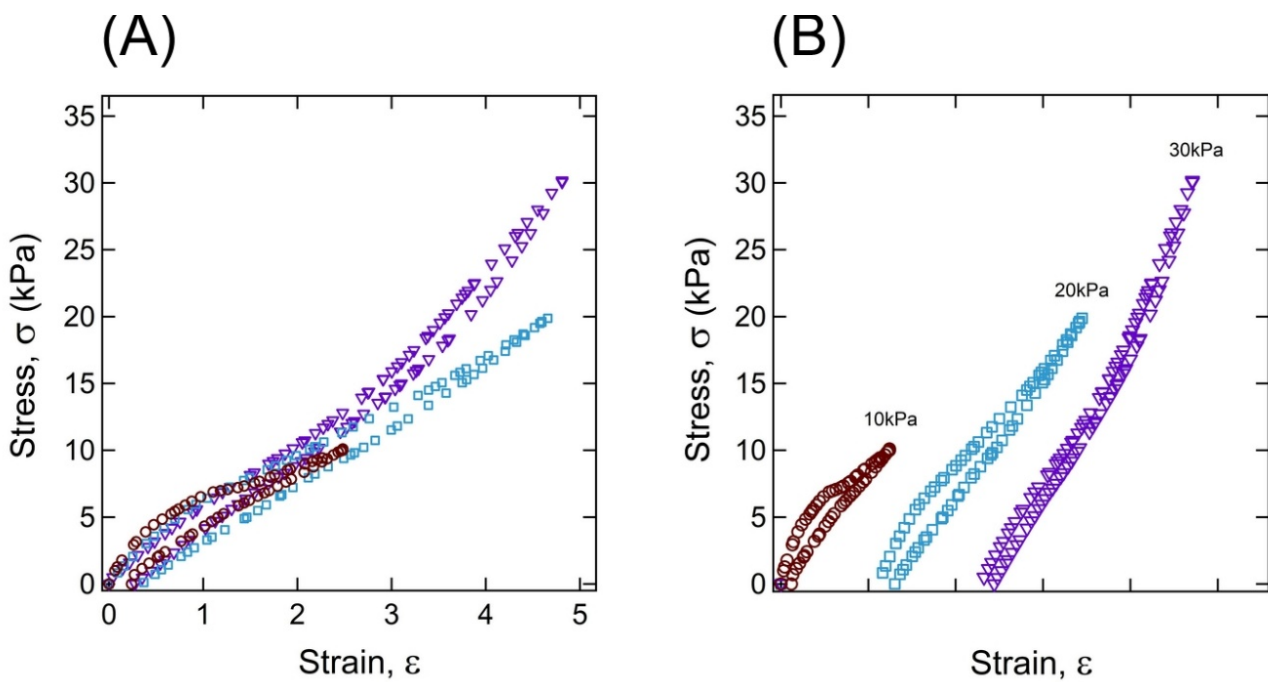
Figure S6. Cyclic loading results of a 17%-Gel. (A) Nominal stress (σ) as a function of strain (ε) obtained from cyclic loading of 10, 20, and 30 kPa. (B) Cycles are moved along the ε-axis for clarity and visualization.
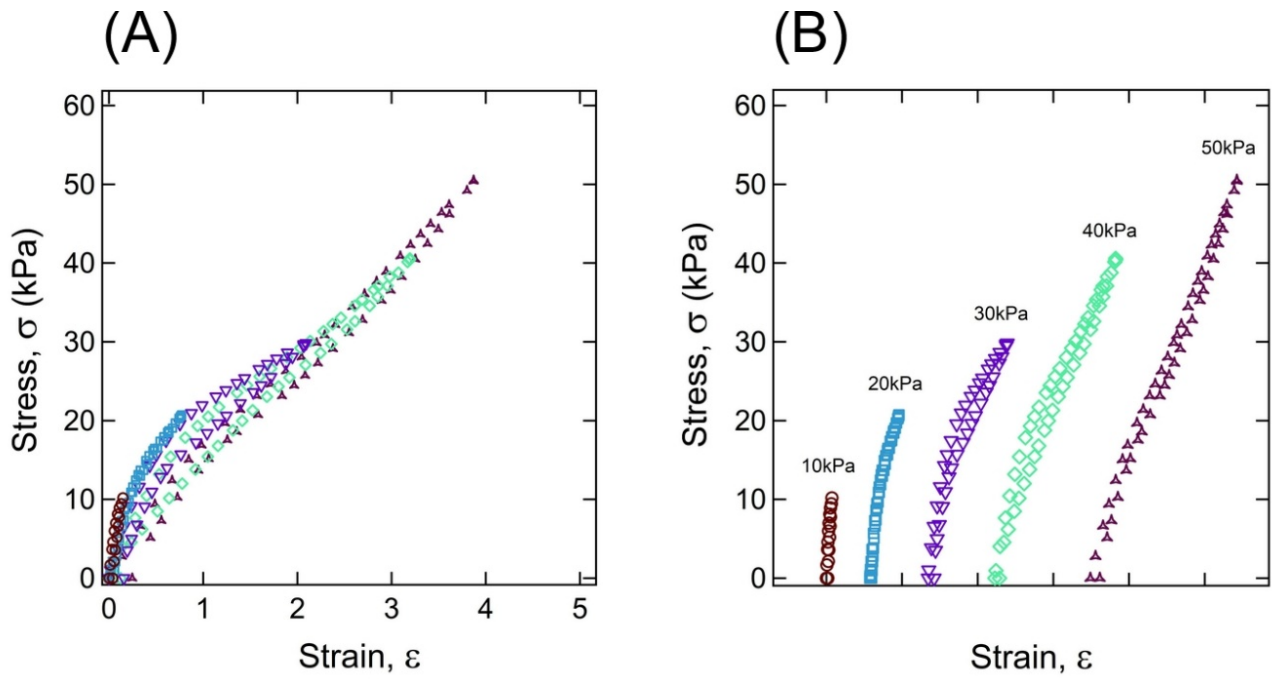
Figure S7. Cyclic loading results of a 27%-Gel. (A) Nominal stress (σ) as a function of strain (ε) obtained from cyclic loading of 10, 20, 30, 40, and 50 kPa. (B) Cycles are moved along the ε-axis for clarity and visualization.
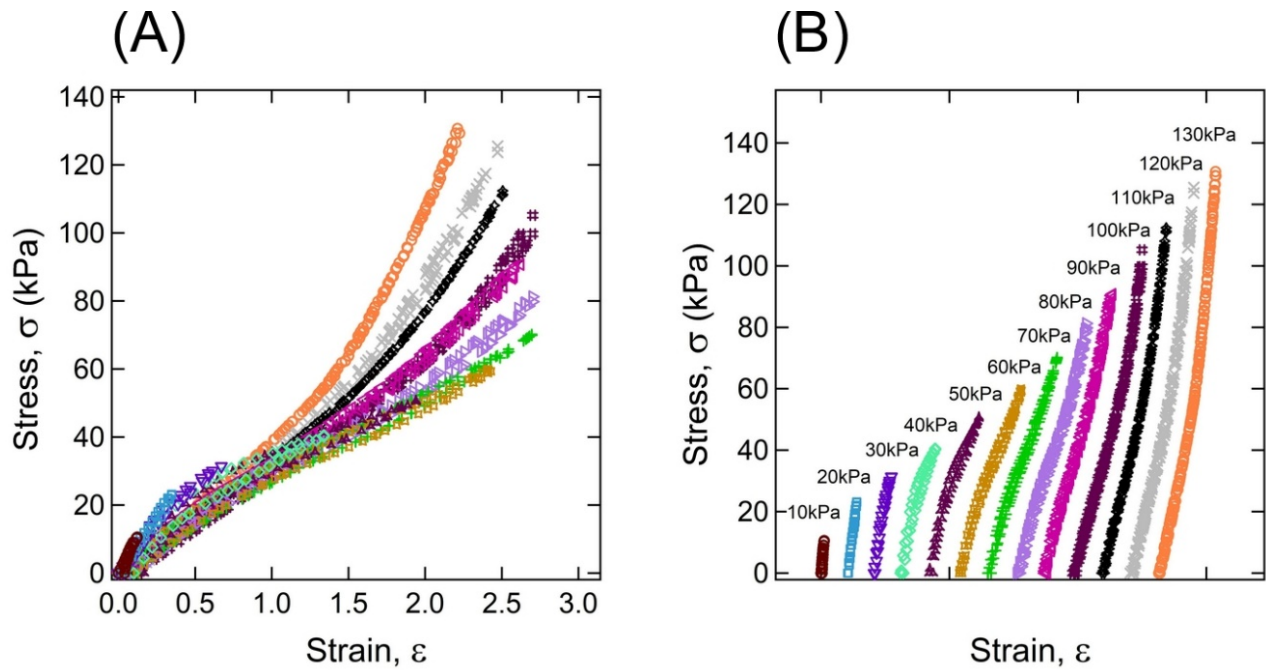
Figure S8. Cyclic loading results of a 37%-Gel. (A) Nominal stress (σ) as a function of strain (ε) obtained from cyclic loading of 10-130 kPa with a step of 10 kPa. (B) Cycles are moved along the ε-axis for clarity and visualization.
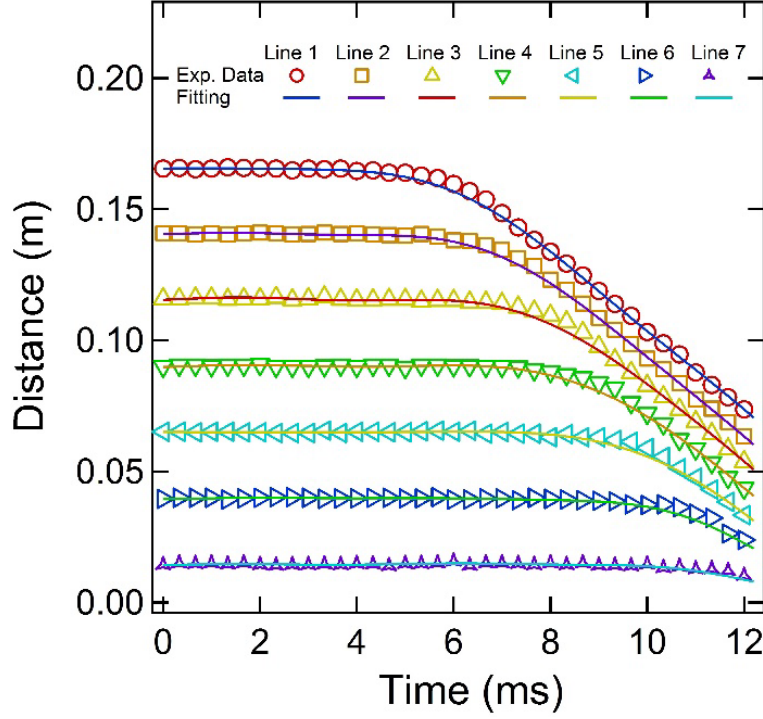
Figure S9. Line positions as a function of time during retraction. The positions of seven marked lines on the samples as a function of time from retraction experiments with λ=6 for a 37%-Gel sample. The symbols display the values obtained from image processing, and the lines indicate the fifth-order Fourier fit.

The position (f) vs. time (t) data of all lines was fitted with the fifth-order Fourier series expressed as, $f(t) = a_0 + \sum_{i=1}^{5} a_i \cos(\omega t) + \sum_{i=1}^{5} b_i \sin(\omega t)$. The obtained function was then differentiated to obtain velocity and acceleration. For example, the fitted parameters obtained for Line 1 for the 37%-Gel (Figure S9) at λ=6 are a_0=-1.521e+08, a_1=2.359e+08, a_2=-1.056e+08, a_3=2.237e+07, a_4=-1.064e+05, a_5=-5.319e+05, b_1=9.706e+07, b_2=-1.046e+08, b_3=5.302e+07, b_4=-1.338e+07, b_5=1.315e+06, and ω=40.32. The value of ω provides a time scale of 156 ms. The total time of the retraction experiment was 18 ms, much lower than the experimental time scale, therefore, this ω value is appropriate for fitting the data.

Table S1. Results of swelling behavior of gels. The results indicate the water content in as-prepared gels and the swelling water capacity.

Sample	Water content in as-prepared samples [%, g g^{-1}]	Swelling ratio after swell in water [g g^{-1}]
17%-Gel	80.9±0.9	87.9±14.9
27%-Gel	67.6±0.2	44.2±1.4
37%-Gel	64.9±0.1	34.6±0.1

Table S2. Resilience of gels. Maximum stress, strain, and resilience (%) values for 17%-, 27%-, and 37%-Gels corresponding to the highest stress cycle applied during cyclic-loading experiments.

Sample	Maximum stress [kPa]	Maximum strain	Resilience [%]
17%-Gel	30	4.8	88.6
27%-Gel	50	3.9	90.3
37%-Gel	130	2.2	97.7

References

(1)   Dubey, S.; Bajpai, S. K. Poly(Methacrylamide-Co-Acrylic Acid) Hydrogels for Gastrointestinal Delivery of Theophylline. I. Swelling Characterization. *J. Appl. Polym. Sci.* **2006**, *101* (5), 2995–3008. https://doi.org/10.1002/app.23542.

(2)   Zhang, F.; Guo, Z.; Gao, H.; Li, Y.; Ren, L.; Shi, L.; Wang, L. Synthesis and Properties of Sepiolite/Poly (Acrylic Acid-Co-Acrylamide) Nanocomposites. *Polym. Bull.* **2005**, *55* (6), 419–428. https://doi.org/10.1007/s00289-005-0458-2.

(3)   Millipore Sigma. IR Spectrum Table and Chart https://www.sigmaaldrich.com/technical-documents/articles/biology/ir-spectrum-table.html (accessed Jun 28, 2020).